

# Bond Graph Modeling of Planar Two Links Flexible Space Robot

P.M. Pathak<sup>1\*</sup>, Amit Kumar<sup>2</sup>, and N. Sukavanam<sup>2</sup>  
<sup>1</sup>Department of Mechanical and Industrial Engineering,  
Indian Institute of Technology, Roorkee, INDIA  
<sup>2</sup>Department of Mathematics, Indian Institute of Technology, Roorkee, INDIA  
\*Corresponding author (email: pushpfme@iitr.ernet.in)

## Abstract

This paper presents a methodology to analyze dynamics of flexible space robot using bond graph. In case of space robots the position and orientation of the satellite main body may change when the manipulator moves. Motion of the space robots also induces vibrating motions in structurally flexible manipulators. Researchers working on terrestrial flexible robot arms principally have focused on issues such as dynamic modeling and vibration control. In the present work the nonlinear coupling of large rigid body motion and small elastic vibration of the flexible arms of space robot has been taken into consideration in the model.

Bond graphs are used to represent both rigid body and flexible dynamics of each link in a unified manner. The links are modeled as Rayleigh beams. An example of two DOF planer space robots is considered to illustrate the methodology. A planer robot is considered for illustration purpose as simple experiments are possible to validate the modeling and validate various control strategies.

**Keywords:** Flexible space roots, bond graphs, dynamic modeling, control.

## 1. Introduction

The flexible manipulator will be useful for space application due to their light weight, less power requirement, ease of maneuverability and ease of transportability. Because of the light weight, they can be operated at high speed. For flexible manipulators flexibility of manipulator have considerable influence on its dynamic behaviors. The flexibility of the link as well as flexibility of joint affects the overall performance of the system. The control of such flexible manipulator is very much influenced by the non-linear coupling of large rigid body motions and small elastic vibrations. In case of space robots the position and orientation of the satellite main body will change due to manipulator motion. The motion of the space robots also induces vibrating motions in structurally flexible manipulators. Researchers working on terrestrial flexible robot arms principally have focused on issues such as dynamic modeling and vibration control.

Murotsu *et al.* [1,2] proposed control schemes for flexible space manipulator using a virtual rigid manipulator concept. Samanta and Devasia [3] have discussed modeling and control of flexible manipulates using distributed actuator. A technique is presented to analyze the dynamics of flexible manipulators using bond graphs. The nonlinear coupling of large rigid body motion and small elastic vibration of the flexible arms has been taken into consideration in the model. The concept of using distributed piezoelectric transducers for controlling elastic vibration of arms has been incorporated in the analysis. Lichang *et al.* [4] worked on dynamic modeling control and simulation of flexible dual arm space robot based on the Lagrange method and described the elastic deflection by the assumed mode method. The inversion dynamic control method is performed to solve the tracking problem. Pathak *et al.* [5] has discussed impedance control of space robots using passive degree of freedom in controller domain. Senda and Murotsu [6] proposed a methodology for designing stable manipulation variable feedback control of a space robot with flexible links for positioning control to a static target and continuous path tracking control. Zhang and Yu [7] developed the dynamic equations of planar cooperative manipulators with link flexibility in absolute coordinate with the help of Timoshenko beam theory and the finite element method. Taking the actual position of the mass centre of the cooperated object as the boundary condition, the inverse dynamic equation is developed with the load distribution method. Stieber *et al.* [8] addressed the stability and control problems arising in vision based control of flexible space robot where the motion of a robot payload relative to the work space is measured at a considerable distance from the control actuator in the robot joints. Jiang [9] developed a concept of compensability for free floating flexible space robot arms. Using this concept is the end-effector behaviour caused by the link flexural behaviour and the satellite motion in response to the arm motion is considered as errors in the end-effector motion and this error is compensated by the joint behaviour.

The bond graph technique offers flexibility in modeling and formulation of system equations. Systems from diverse branches of engineering can be modeled in a unified manner using bond graph [10]. They represent the power exchange portrait of the system. Power is expressed as multiplication of two factors, generalized effort and generalized flow. In bond graph modeling a modeler di-

vides a system into dynamic units comprised of inertances (I), compliances (C), and dissipations (R). The external source inputs to system are expressed as source of effort (SE) or source of flow (SF) elements. Two multiport elements transformer (TF) and Gyrator (GY), are also used. TF elements perform flow-to-flow or effort-to-effort conversion, whereas GY element converts flow-to-effort or effort-to-flow. Constraints are represented using element 1 (representing constant flow) and element 0 (representing constant effort). The elements are connected by line segments called bonds, which portray the path of exchange of power with in the constraint structure and elements. The notion of causality provides a tool for formulation of system equations.

This paper presents the bond graph modeling of a flexible links space robot. Links are modeled as Rayleigh beam. Bond graphs are used to represent both rigid body and flexible dynamics of each link in a unified manner. SYMBOLS Shakti [11] software is used for bond graph modelling and simulation. An example of two DOF planar space robot is considered to illustrate the methodology. A planar robot is considered for illustration purpose as simple experiments are possible to validate the control strategy.

## 2. Rayleigh Beam Model

In Rayleigh beam model rotary inertia of the beam is taken into account though shear deformation is neglected. In creating Rayleigh beam model finite lumping is done for both mass and rotary inertia. A beam element with shear forces and moments acting on it in Newtonian convention is shown in Fig. 1. The stiffness of the beam element relates the generalised Newtonian force to the generalised displacements at the ends of the element as given by equation (1) as

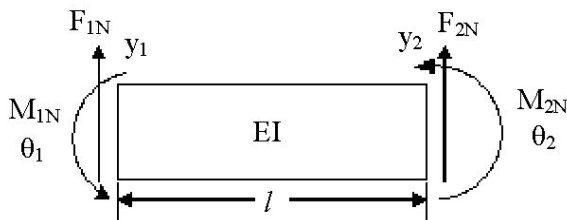


Figure 1. Beam element with generalized forces and displacements

$$\begin{Bmatrix} F_{1N} \\ M_{1N} \\ F_{2N} \\ M_{2N} \end{Bmatrix} = [K] \begin{Bmatrix} y_1 \\ \theta_1 \\ y_2 \\ \theta_2 \end{Bmatrix} \quad (1)$$

The stiffness matrix [K] can be modeled as a 4-port C-field storing energy due to the four generalized displacements as

shown in Fig.2.

Any column of the stiffness matrix can be determined by assigning unit value to the corresponding row element of

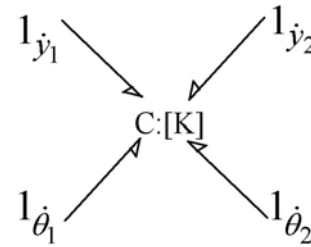


Figure 2: C-field representing the beam element stiffness matrix

the displacement vector, all other elements being zero and then evaluating the equilibrium forces and moments on an element satisfying the Eq. (2) to the elastic line.

$$M(x) = EI \frac{\partial^2}{\partial x^2} y(x) \quad (2)$$

In terms of flexural rigidity  $EI$  and element length  $l$  the stiffness matrix is given by Eq. (3) [10].

$$[K] = \frac{EI}{l^3} \begin{bmatrix} 12 & 6l & -12 & 6l \\ 6l & 4l^2 & -6l & 2l^2 \\ -12 & -6l & 12 & -6l \\ 6l & 2l^2 & -6l & 4l^2 \end{bmatrix} \quad (3)$$

A bond graph model of beam element can now be created by lumping the element inertia at the ends of the element and appending them to the 1-junctions representing displacements and rotations at the ends of the element. Cascading of several elements bond graph modules leads to the space reticulated beam model.

A cantilever beam with reticulation and lumping of inertia is shown in Fig.3. In the bond graph model fixed end lumped inertias will be in differential causality since the flows are determined by the sources satisfying the

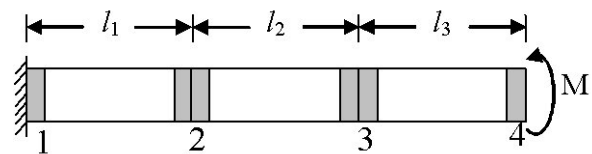


Figure 3: Cantilever beam with space reticulation and inertia lumping

boundary conditions. These can, therefore, be removed. The obtained integrally caused model is shown in Fig. 4.

Lumped linear inertias may be obtained as

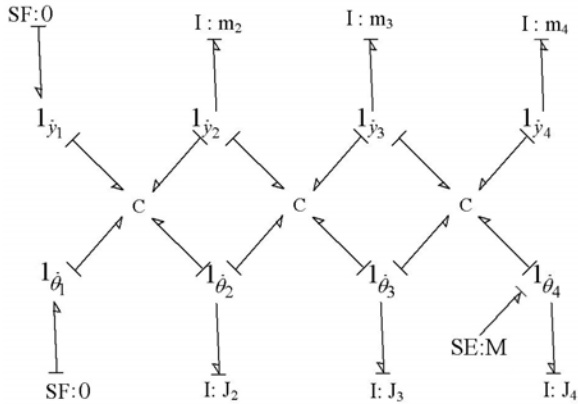


Figure 4: Integrally causalled model for cantilever beam with space reticulation and inertia lumping

$$m_2 = \frac{\rho A(l_1 + l_2)}{2}, \quad m_3 = \frac{\rho A(l_2 + l_3)}{2}, \quad \text{and} \quad m_4 = \frac{\rho A l_3}{2},$$

Where  $\rho$  is density of the material and A is the cross sectional area.

For estimation of lumped rotary inertia let us take a beam element of the length  $\Delta x$ , width b and height h as shown in Fig.5, the moment equation in difference form is given by

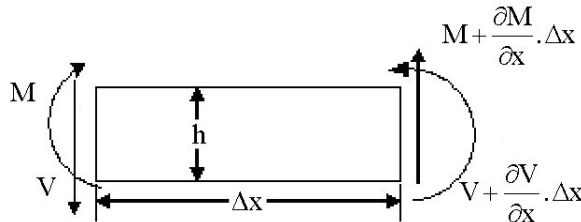


Figure 5: Beam element for evaluation of lumped rotary inertia

$$\frac{\partial M}{\partial x} \Delta x + V \Delta x + \frac{\partial V}{\partial x} \frac{\Delta x^2}{2} = \left( \frac{\rho b h \cdot \Delta x}{12} \right) (h^2 + \Delta x^2) \frac{\partial^3}{\partial x \partial t^2} y(x, t) \quad (4)$$

Dividing both sides of Eq. (4) by  $\Delta x$  and taking limit  $\Delta x \rightarrow 0$

$$\frac{\partial M}{\partial x} + V = \left( \frac{\rho b h^3}{12} \right) \frac{\partial^3}{\partial x \partial t^2} y(x, t) \quad (5)$$

$$\frac{\partial M}{\partial x} + V = \rho I \frac{\partial^3}{\partial x \partial t^2} y(x, t) \quad (6)$$

where I is the second moment of the beam cross sectional area about neutral axis .

Taking analogy from Eq. (6) rotary inertia may be lumped as follows

$$J_2 = \rho I \frac{(l_1 + l_2)}{2}, \quad J_3 = \rho I \frac{(l_2 + l_3)}{2}, \quad \text{and} \quad J_4 = \rho I \frac{l_3}{2}.$$

### 3. Modelling of Flexible Space Robot

The modeling of the space robot involves the modeling for linear and rotational dynamics of the links and the base of space robot. In space robot modeling it is assumed that the system has single manipulator with revolute joints and is

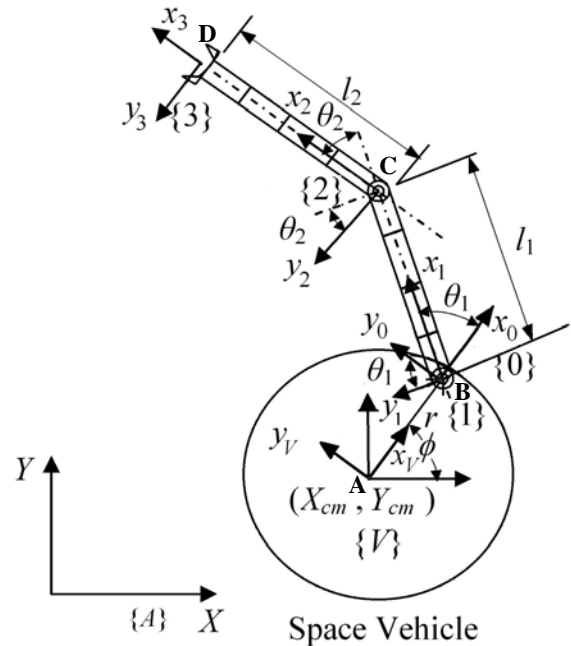


Figure 6. Schematic diagram of 2 DOF flexible planar space robot

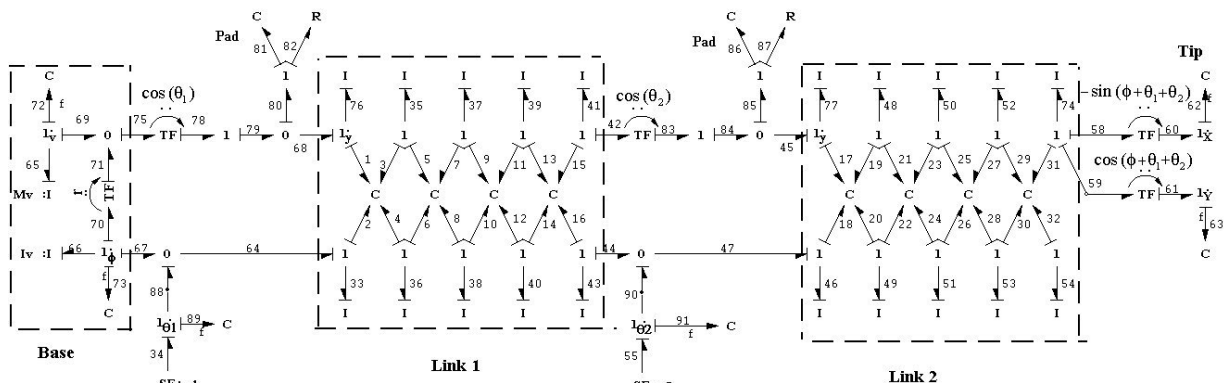


Figure 7. Bond graph model of flexible space robot

in open kinematic chain configuration. Figure 6 shows the schematic sketch of a two DOF planar flexible space robot. In this figure  $\{A\}$  represents the absolute frame,  $\{V\}$  represents the vehicle frame,  $\{0\}$  frame is located at the base of the robot,  $\{1\}$ ,  $\{2\}$  are the frames located at first and second joint respectively. The frame  $\{3\}$  locates the tip of the robot. Let  $l_1$  be the length of the first link,  $l_2$  be the length of second link and  $r$  be the distance between the robot base and CM of the vehicle. Let  $\phi$  represent the rotation of vehicle frame with respect to an absolute frame, and  $\theta_1$ , and  $\theta_2$  be the joint angles as shown in Fig 6. Let the first motor is mounted on base and has a mass  $m_1$  and it applies a torque  $\tau_1$  on first link. Similarly let the second motor is mounted on first link. It has a mass  $m_2$  and it applies a torque  $\tau_2$  on second link. The links are uniform with flexible rigidities  $EI_1$  and  $EI_2$  and cross section area  $A_1$  and  $A_2$  respectively.

The kinematic analysis of the different links is performed in order to draw the bond graph as shown in Fig. 7. From the kinematic relations the different transformer modulli used in the bond graph are derived. The lengths of the links are divided into four equal segments. Each segment of the link is represented by a C field element. Two types of motion of the links are considered. First motion is the motion perpendicular to link, and second motion is the rotational motion of links. Pads are used for computational simplicity i.e. to avoid the differential causality [10]. Tip velocities are calculated in X and Y direction to observe tip motion in XY plane.

#### 4. Simulation and Results

Table 1 shows the data used for simulation of flexible link space robot. The links are assumed to be made of aluminum. The initial values of  $\phi$ ,  $\theta_1$ , and  $\theta_2$  are assumed to be 0.1 rad, 0.2 rad and 0.3 rad. Simulation is performed for 10 sec. The simulation is carried for two cases, (i) with no joint control (ii) with joint control.

##### (i) With no joint control

For this case the applied input joint torque to first and second joint are given as,

$$\tau_1 = T_1 \cos(\omega t)$$

$$\tau_2 = T_2 \cos(\omega t)$$

The assumed values of  $T_1$  and  $T_2$  are 0.4 Nm and 0.2 Nm respectively. The  $\omega$  is taken as 2.0 rad/s. The values used in simulation are shown in Table 1. The simulated results are shown in Fig. 8. Figure 8(a) shows the variation of first and second joint angle with time. It is seen from the Fig. that the first and second joint have oscillatory motion from their initial position of 0.2 rad and 0.3 rad. Fig. 8(b) shows the base rotation, because of the joint movement. Figure 8 (c) shows the variation of the tip position in X and Y direc-

tion with respect to time. Figure 8(d) shows the tip plot in

Table 1: Parameters used in simulation

Parameter	Value
Modulus of Elasticity	$E=71 \times 10^9 \text{ N/m}^2$
First link length	$L_1 = 0.5 \text{ m}$
Second link length	$L_2 = 0.6 \text{ m}$
Moment of inertia of cross section of first link	$I_1=1.256e-7 \text{ m}^4$
Moment of inertia of cross section of second link	$I_2=1.256e-7 \text{ m}^4$
Density of Aluminum	$P= 2700 \text{ Kg/m}^3$
Cross section area of first link	$A_1=0.00125 \text{ m}^2$
Cross section area of second link	$A_2=0.00125 \text{ m}^2$
Mass of first motor	$m_1 = 0.1 \text{ Kg}$
Mass of second motor	$m_2= 0.1 \text{ Kg}$
Proportional gain used in control law for joint angle control	$K_p = 4.0$
Derivative gain used in control law for joint angle control	$K_v = 3.0$
Desired angle for first joint	$\theta_{1d} = 0.5 \text{ rad}$
Desired angle for second joint	$\theta_{2d} = 0.6 \text{ rad}$
Mass of the base	$M_b = 5.0 \text{ Kg}$
Polar moment of inertia of base	$J_b = 0.025 \text{ m}^2$
Radius of base	$r = 0.1 \text{ m}$

X-Y plane.

##### (ii) With joint control

A PD controller is used to control the two joints. The control law used for joint control is given as

$$\tau_1 = K_{p1} (\theta_{1d} - \theta_{1a}) + K_{v1} (\dot{\theta}_{1d} - \dot{\theta}_{1a})$$

$$\tau_2 = K_{p2} (\theta_{2d} - \theta_{2a}) + K_{v2} (\dot{\theta}_{2d} - \dot{\theta}_{2a})$$

Here  $\theta_{1d}$ , and  $\theta_{2d}$  are desired first and second joint angles whereas  $\theta_{1a}$ , and  $\theta_{2a}$  are actual values of first and second joint angles,  $K_{p1}$  and  $K_{p2}$  are proportional gains,  $K_{v1}$  and  $K_{v2}$  are the derivative gains. The values used in simulation are shown in Table 1.

Figure 9(a) shows the variation of first and second joint angle with time. It is seen from the Fig. that the first and second joint reaches to desired location of 0.6 rad and 0.8 rad from 0.2 rad and 0.3 rad respectively. Fig. 9(b) shows the base rotation, because of the joint movement. It is because the system is a non holonomic. This attitude

disturbance however can be restored by attitude control devices. Figure 9 (c) shows the variation of the tip position in X and Y direction with respect to time. Figure 9(d)

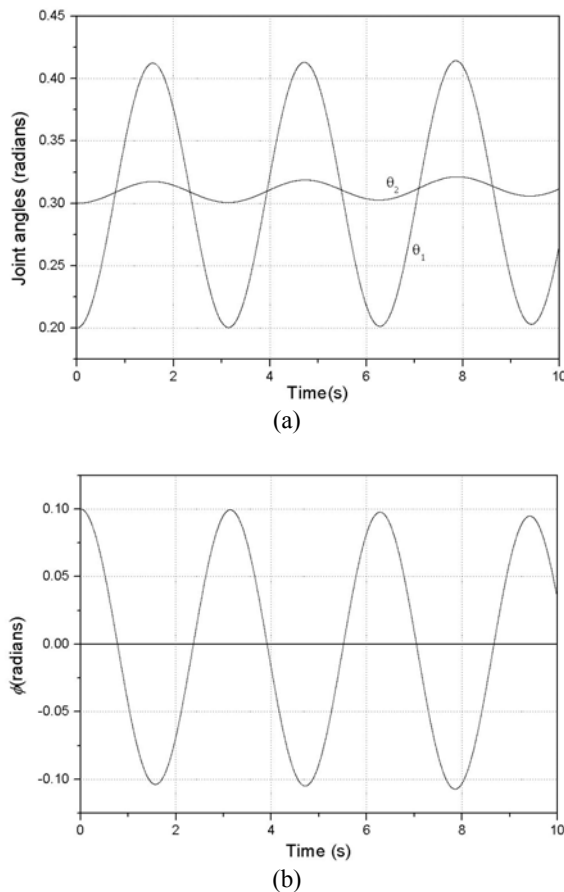


Figure 8 (a) Variation of first and second joint angle with time without joint motion control. (b).Variation of base rotation with time without joint motion control

shows the tip plot in X-Y plane.

## 5. Conclusions

The bond graph modeling of space robot with flexible link is presented in the paper. Links are modeled as Rayleigh beam. A simple PD control is used for the two joints. The aim the work is to prepare a model for flexible space robot which can be subsequently used for trajectory control/impedance control strategies.

## References

[1] Y. Murotsu, S. Tsujio, K. Senda and M. Hayashi, "Trajectory control of flexible manipulators on a free flying space robot", IEEE Control systems, 1992, pp. 51-57.

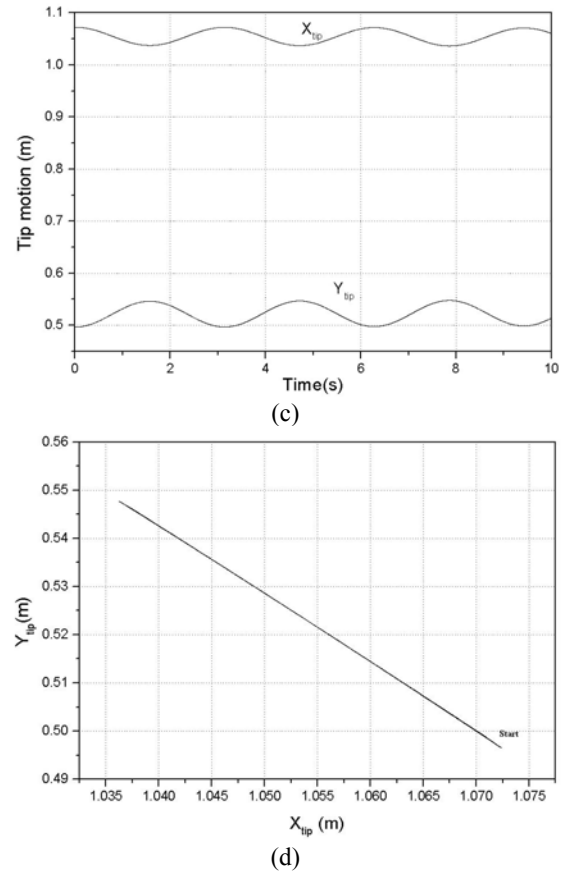


Figure 8 (c) Variation of the tip position in X and Y direction with respect to time without joint motion control. (d) Tip plot in X-Y plane without joint motion control

[2] Y. Murotsu, K. Senda and M. Hayashi, "Some trajectory control schemes for flexible manipulators on a free flying space robot", Proceedings of International conference on intelligent robots and systems, Raleigh 1992, pp.1697-1704.

[3] B. Samanta and S. Devasia, "Modelling and control of flexible manipulators using distributed actuators: a bond graph approach", Proceedings of the IEEE International Workshop on Intelligent Robots and Systems, 1988, pp. 99-104.

[4] W. Licheng, S. Fuchun, S. Zengqi and S. Wenjing, "Dynamic modeling control and simulation of flexible dual arm space robot", Proceedings of IEEE TENCON, 2002, pp.1282-1285.

[5] P.M. Pathak, A. Mukherjee, A. Dasgupta" Impedance Control of Space Robots Using Passive Degrees of Freedom in Controller Domain ", Transactions of the ASME, Vol. 127, 2005, pp. 564-578.

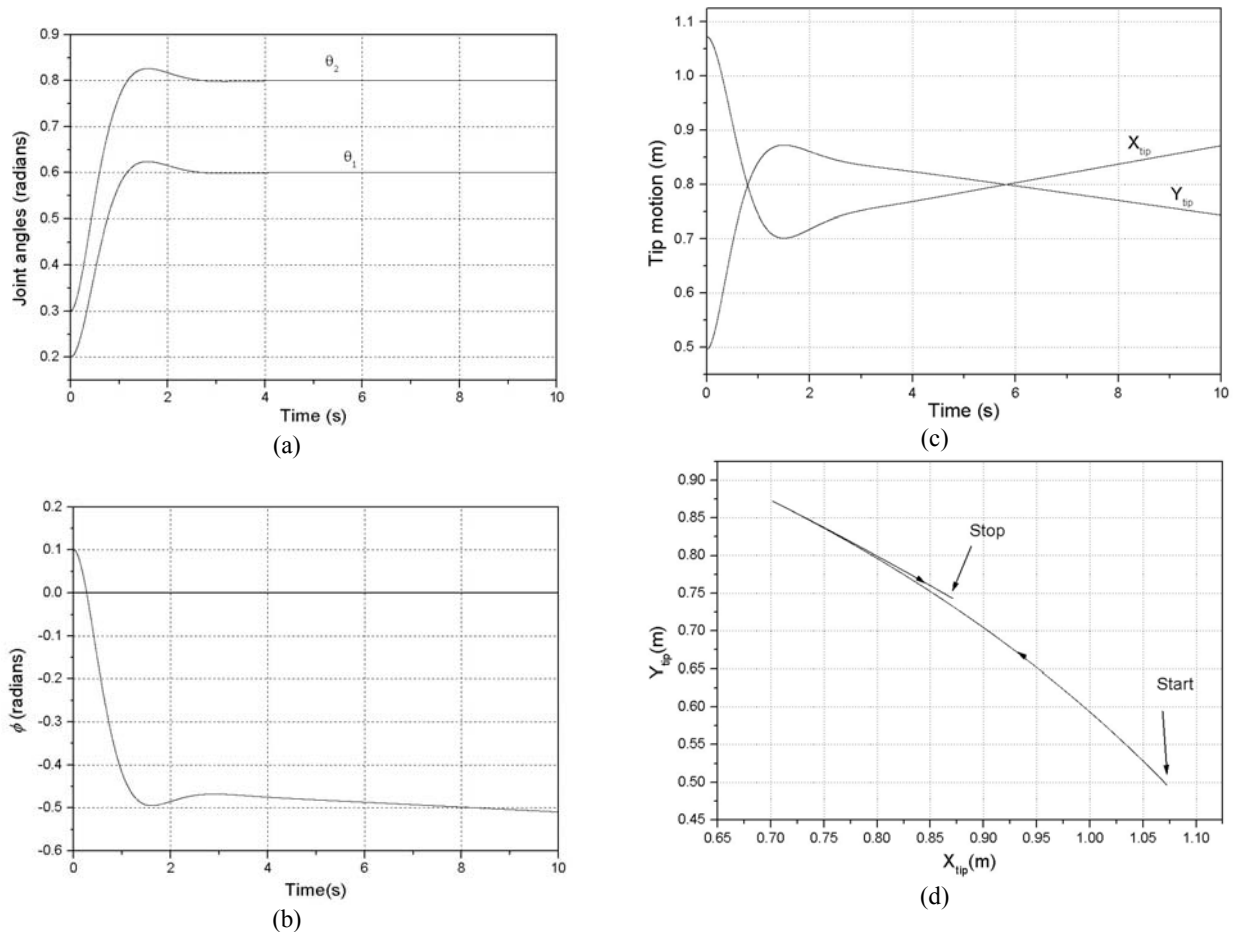


Figure 9 (a) Variation of first and second joint angle with time with joint motion control. (b).Variation of base rotation with time with joint motion control

Figure 9 (c) Variation of the tip position in X and Y direction with respect to time with joint motion control. (d) Tip plot in X-Y plane with joint motion control.

[6] K.Senda and Y. Murotsu, "Methodology for control of a space robot with flexible links", IEE Proc. Control Theory Appl., Vol. 147, No. 6, 2000, pp. 562-568.

[7] C. Zhang, and Y.Q. Yu, "Dynamic analysis of planar cooperative manipulators with link flexibility", Transactions of ASME, Vol. 126, 2004, pp. 442-448.

[8] M.E. Stieber, G.Vukovich, and E. Petriu, "Stability aspects of vision based control for space robots", Proceedings of the 1997 IEEE International conference on Robotics and Automation, Albuquerque, New Mexico, 1997, pp. 2771-2776.

[9] Z.H.Jiang, "Compenstability of end-effector motion errors and evaluation of manipulability for flexible space robot arms", IEEE International conference on Systems, Man and Cybernetics, 1992, pp.486-491.

[10] A. Mukherjee, and R. Karmakar, and A. K. Samantaray, Bond Graph in Modeling, Simulation and Fault Identification. New Delhi: I. K. International Publishing House Pvt. Ltd, 2006, CRC press; 2nd edition (2006)

[11] Users Manual of SYMBOLS Shakti, <http://www.htcinfo.com/>, High-Tech Consultants, S.T.E.P., Indian Institute of Technology, Kharagpur (2006).